Approximate Computation of Heat Sources in Axisymmetric Microwave Heating

M. Kostoglou and T. D. Karapantsios
Division of Chemical Technology, Dept. of Chemistry, Aristotle University, 541 24 Thessaloniki, Greece

DOI 10.1002/aic.10636
Published online September 1, 2005 in Wiley InterScience (www.interscience.wiley.com).

Keywords: microwave heating, cylindrical geometry, radial irradiation, Maxwell equations, Lambert law

Introduction

Microwave radiation offers the very important feature of inducing volumetric heating in a sample that leads to faster processing rates and lower thermal gradients in the heated material than the conventional techniques based on boundary heating. This feature has led to the use of microwaves as heating means in many practical applications, especially related to food technology. Given the importance of microwave heating, the abundance of reported studies in the literature regarding its modeling is not surprising.

Microwaves create very complex heat source patterns in the heated material. These patterns can be found from the solution of the Maxwell equations. Although their two- (2D) and three-dimensional (3D) solutions are feasible[1] (but computationally demanding), the one-dimensional (1D) case is usually invoked to attain greater insight on the physics of the problem. The usual 1D approximation refers to the normally irradiated slab[2,3] (Cartesian geometry) and the radially irradiated cylindrical sample (axisymmetric case). The latter 1D model has been used to simulate the heating of cylindrical samples in actual microwave ovens based on the dubious assumption that multiple reflections from the oven's wall lead to an approximately 1D pattern in the sample.[4] Recently, it has been experimentally shown that the temperature profile in a rotated cylindrical sample is axisymmetric so the radially irradiated model is appropriate for this case.[5]

Correspondence concerning this article should be addressed to M. Kostoglou at kostoglu@chem.auth.gr.

The heat source patterns resulting from the Maxwell equations for the 1D case are not so simple, especially for the case of nonuniform dielectric properties for which a numerical solution is needed. For this reason, several simple expressions for heat sources based on Lambert's law have been proposed. Although the limits of validity of these expressions for the case of an 1D slab have been extensively studied years ago,[6] only recently have the corresponding limits for the axisymmetric geometry been proposed.[7] In the present work, the approximate expressions for the heat sources in a radially irradiated cylindrical sample are reviewed and the corresponding validity region for the best one (much wider than that proposed previously[7]) is given. In addition, criteria for the application of simplified expressions for sources in the case of temperature-dependent dielectric properties are presented for the first time.

Problem Formulation

The electric field intensity is a complex quantity with real and imaginary parts, E_R and E_I, respectively (that is, $\mathbf{E} = E_R + iE_I$, where bold characters refer to complex variables). Its spatial distribution with respect to the radial coordinate r can be found from the solution of the following equations (which result from the Maxwell equations by assuming a harmonic time dependency of the electric field[7]):

$$\frac{\partial^2 E_R}{\partial r^2} + \frac{1}{r}\frac{\partial E_R}{\partial r} + \left(\frac{2\pi f}{c}\right)^2 \kappa' E_R - \left(\frac{2\pi f}{c}\right)^2 \kappa'' E_I = 0 \quad (1)$$

$$\frac{\partial^2 E_I}{\partial r^2} + \frac{1}{r}\frac{\partial E_I}{\partial r} + \left(\frac{2\pi f}{c}\right)^2 \kappa' E_I + \left(\frac{2\pi f}{c}\right)^2 \kappa'' E_R = 0 \quad (2)$$

with the following boundary conditions:

Axial Symmetry

$$\frac{\partial E_R}{\partial r} = \frac{\partial E_I}{\partial r} = 0 \qquad \text{at } r = 0 \tag{3}$$

Radiation Boundary Condition

$$\frac{\partial E_R}{\partial r} + C_{1R}E_R - C_{1I}E_I = C_{2R} \qquad \text{at } r = R \tag{4}$$

$$\frac{\partial E_I}{\partial r} + C_{1R}E_I + C_{1I}E_R = C_{2I} \qquad \text{at } r = R \tag{5}$$

where

$$\mathbf{C}_1 = C_{1R} + iC_{1I} = x\frac{J_1(x)J_0(x) + Y_1(x)Y_0(x)}{J_0^2(x) + Y_0^2(x)} + i\frac{2}{\pi[J_0^2(x) + Y_0^2(x)]} \tag{6}$$

$$\mathbf{C}_2 = C_{2R} + iC_{2I} = \frac{4Y_0(x)E_0}{\pi[J_0^2(x) + Y_0^2(x)]} + i\frac{4J_0(x)E_0}{\pi[J_0^2(x) + Y_0^2(x)]} \tag{7}$$

$$x = \frac{2\pi fR}{c} \tag{8}$$

and J_0, J_1, Y_0, and Y_1 are the zero- and first-order Bessel functions of the first and second kind, respectively. The relative dielectric constant κ' and relative dielectric loss κ'' of the radiated material appear in Eqs. 1 and 2.

The volumetric heat generation rate Q is equal to the radiation power dissipated in the medium and can be found as

$$Q = \pi f\varepsilon_0\kappa''(E_R^2 + E_I^2) \tag{9}$$

In the above equations, R is the radius of the cylindrical sample, f is the microwave radiation frequency, c is the speed of light, ε_0 is the free space permittivity, and E_0 is the intensity of the incident radiation.

For constant dielectric properties, the above system has an analytical solution in terms of Bessel functions with complex arguments.[7] In this case, the analytical solution is used for the subsequent computations. In any other case, the system is solved using a shooting procedure. The unknown variables are the values of the field at the symmetry axis, $E_R(0)$, $E_I(0)$. A value is assumed for these variables and the system of Eqs. 1 and 2 is integrated as an initial-value problem using an explicit Runge–Kutta integrator with self-adjusting step size and arbitrary specified accuracy.[8] If the solution does not satisfy the boundary conditions 4 and 5 a new estimation of $E_R(0)$, $E_I(0)$ is taken through a Newton–Raphson procedure. The above procedure is repeated until convergence is achieved.

Heat source approximations

Several approximate forms have been proposed for Q based on Lambert law. According to this law, the variation of the transmitted power flux I with distance z from the sample surface is

$$I(z) = I_0e^{-2\beta z} \tag{10}$$

where

$$\beta = \frac{2\pi f}{c}\sqrt{\frac{\sqrt{\kappa'^2 + \kappa''^2} - \kappa'}{2}} \tag{11}$$

and I_0 is the incident power flux on the surface of the sample.

Based on this law, Oliveira and Franca[7] used the following expression for Q for radial irradiation of a cylindrical sample:

$$Q_1(r) = 2I_0\beta e^{-2\beta(R-r)} \tag{12}$$

The above expression is similar to that used for rectangular geometry[6] and ignores the densification of the adsorbed energy toward the center of the sample.

Performing a careful balance between the entering, produced, and exiting power for a cylindrical shell of infinitesimal thickness, Chen et al.[9] proposed the following relation:

$$Q_2(r) = 2I_0\beta\frac{R}{r}e^{-2\beta(R-r)} \tag{13}$$

Finally, Lin et al.[10] modified the above relation by taking into account the contribution of the radiation entering to the sample from the antidiametrical point:

$$Q_3(r) = 2I_0\beta\frac{R}{r}[e^{-2\beta(R-r)} + e^{-2\beta(R+r)}] \tag{14}$$

In the above equations, β can be a strong function of temperature and, consequently, spatial dependent. For example, β for water falls to its half value as the temperature goes from 20 to 50°C. In such a case, however, it is not reasonable that the local radiation intensity depends only on the local value of β and not on the β-values along its previous path. A closer examination of the physics of the problem reveals that a running integral over β is more appropriate:

$$Q_4(r) = 2I_0\beta(T)\frac{R}{r}e^{-2\int_r^R \beta dr} \tag{15}$$

The use of Eq. 15 is not so popular in the literature and Eq. 13 is still heavily used even for cases where the temperature dependency of dielectric properties is a major aspect of the whole process.[11] Expressions analogous to Eq. 15 can also be developed on the basis of Eq. 14.

It is noted that all the above approximate forms of the Q value exhibit a singularity of type $1/r$ at the center of the cylinder $r = 0$. This is not a severe problem because it corresponds to a finite slope of the temperature profile at $r = 0$ [that

is, $(\partial T/\partial r)_{r=0} \neq 0$]. By setting an upper limit to Q values (cutoff value) the temperature slope at $r = 0$ will go to zero with only a small (local) influence in the temperature profile. Nevertheless, the singularity of Q creates problems to the numerical solution of the heat-transfer equation.

Results and Discussion

The length $1/\beta$ is called penetration length and represents the thickness of the sample penetrated effectively by radiation. For the case of a characteristic sample dimension much larger than the penetration depth, a monotonic function $Q(r)$ (which can be easily approximated by Lambert's law) results from the solution of Maxwell's equations. As the ratio of the characteristic sample size to penetration depth (βR) decreases, the function $Q(r)$ becomes increasingly more oscillated with local peaks and valleys.[2] This shape cannot be approximated by Lambert's law. The value of the above ratio at which the Lambert's law diverges from Maxwell's equation has been found[6] to be 2.7 for the slab geometry (characteristic dimension is the thickness of the slab). Recently,[7] a similar analysis has been performed for a radially irradiated cylinder and the critical ratio was determined to be $\beta R = 7$. This value precludes any practical use of Lambert's law for cylindrically shaped samples.

To perform an analysis of the above type for the assessment of an approximate formula for $Q(r)$, some specific points must be clarified. First of all, a matching procedure for the parameters E_0 and I_0 must be defined. Their fundamental relation in free space [$I_0 = (1/2)c\varepsilon_0 E_0^2$] leads to very poor results.[12] The procedure followed by Ayappa et al.[6] consists of equating the exact and approximate expressions of Q for the case of a semi-infinite slab. In Oliveira and Franca,[7] the matching condition (as inferred from their figures) is $Q(R) = Q_1(R)$. Second, an appropriate error norm must be defined. This norm is the square root of the average of the second power of the difference between Q and Q_1 divided by $Q_1(R)/2$ for the planar geometry[6] and $Q_1(R)$ for the cylindrical geometry.[7] The criterion for the evaluation of the critical ratio is that the above norms must be equal to 0.01.

The analysis for the cylindrical geometry case exhibits several subtle points, which are believed to be the reason for the particular large value of the critical ratio, $\beta R = 7$, derived by Oliveira and Franca.[7] First, it is based on the approximation Q_1, which is not an acceptable form of Lambert's law for the cylindrical geometry. Second, the nonnormalized error norm that is used,

$$\sqrt{\frac{1}{R}\int_0^R (Q - Q_1)^2 dr} \tag{16}$$

does not have a clear physical meaning. The correct volumetric average of the square of the deviation between the two relations is defined as

$$\sqrt{\frac{2}{R^2}\int_0^R r(Q - Q_1)^2 dr} \tag{17}$$

Also, the applied matching procedure between the two relations in Oliveira and Franca[7] is not a good choice. Here, the above weak points are relaxed as follows: the approximate relations Q_2, Q_3, and Q_4 are used instead of Q_1. A new matching procedure is introduced according to which the approximate average heat generation rate must be equal to the corresponding exact one. This means that the comparison must be made between the following dimensionless relations:

$$Q_d = \frac{R^2 Q}{2\int_0^R rQ dr} \tag{18}$$

$$Q_{2d} = \frac{R^2}{2r}\frac{e^{2\beta r}}{\int_0^R e^{2\beta r} dr} \tag{19}$$

$$Q_{3d} = \frac{R^2}{2r}\frac{e^{-2\beta(R-r)} + e^{-2\beta(R+r)}}{\int_0^R (e^{-2\beta(R-r)} + e^{-2\beta(R+r)}) dr} \tag{20}$$

$$Q_{4d} = \frac{R^2}{2r}\frac{\beta e^{-2\int_r^R \beta dr}}{\int_0^R \beta e^{-2\int_r^R \beta dr} dr} \tag{21}$$

In the particular case of β being constant, $Q_{4d} = Q_{2d}$ and the integrations in Eqs. 19 and 20 can be performed analytically, so that

$$Q_{2d} = \frac{R^2\beta}{r}\frac{e^{2\beta r}}{e^{2\beta r} - 1} \tag{22}$$

$$Q_{3d} = \frac{R^2\beta}{r}\frac{e^{-2\beta(R-r)} + e^{-2\beta(R+r)}}{1 - e^{-4\beta r}} \tag{23}$$

The error norm is normalized with respect to the average heat generation rate. The approximate expressions Q_2 and Q_3 diverge in a rate proportional to $1/r$ at $r = 0$. This has as a result the divergence of the error norm (Eq. 17), which is based on the square of the deviation. A different error norm based on the absolute value of the deviations is the appropriate one for the present case. Summarizing the above, the error norms used here are ($i = 2, 3, 4$)

$$N_i = \frac{2}{R^2}\int_0^R r|Q_d - Q_{id}| dr \tag{24}$$

Uniform dielectric properties

A very important outcome of the analysis performed by Ayappa et al.[6] and Oliveira and Franca[7]—for a large variety of foods and several values of microwave frequencies and tem-

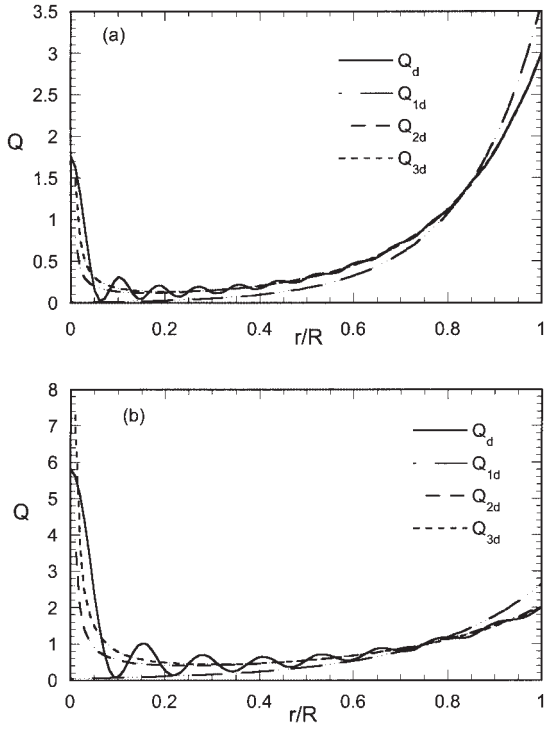

Figure 1. Exact and approximate normalized distribution of the heat source.

Water at $f = 2750$ MHz, $T = 25$°C: (a) $\beta R = 3$; (b) $\beta R = 2$.

peratures—is that the performance of Lambert's law depends only on the dimensionless ratio βR and not on the individual parameters (κ', κ'', f, R). This means that to perform a similar analysis, examination of a certain food material under a certain set of conditions is sufficient. Here, pure water is examined for $f = 2750$ MHz and $T = 25$°C, choices dictated by the main interest in this laboratory regarding microwaves technology and, in particular, microwave gelatinization of dilute starch/water mixtures[13] that have dielectric properties in close proximity to those of water.[14]

According to the computations, the values of error norm N_2 for constant β can be fitted using the equation

$$N_2 = \exp[-0.031927 - 0.76089\beta R - 0.23398(\beta R)^2 + 0.017808(\beta R)^3] \quad (25)$$

The norm N_3 is always slightly smaller than N_2, with the difference to increase as βR decreases. For $\beta R = 1$, $N_2 = 0.365$ and $N_3 = 0.347$ but for values of βR small enough for the approximations to be valid, N_2 and N_3 are extremely close. We focus on the approximation Q_2 because of its simpler form and wider use. It is noteworthy that the error is only 2% for a value of βR as small as 3, which is too far from the value 7 (the critical value of βR proposed by Oliveira and Franca[7]). The reason for this discrepancy becomes clear when examining the form of the function $Q(r)$ shown in Figures 1a and 1b for $\beta R = 3$ and 2, respectively. As βR decreases, more profound oscillations appear in $Q(r)$ with a (finite height) spike at $r = 0$. Approximations Q_2 and Q_3 (in contrast to Q_1) can approximate this spike by their diverging behavior at $r = 0$. In addition, it is seen that the main divergence between exact and approximate forms of $Q(r)$ is in the region of small r. This region has a very small contribution to the correct error norm (Eq. 17, weighted with respect to r), leading to much smaller values than the error norm (Eq. 16). For completeness, the dimensionless form of the rather disappointing approximation Q_1

$$Q_{1d} = \frac{R^2}{2}\frac{e^{2\beta r}}{\int_0^R re^{2\beta r}dr}$$

is also shown in Figure 1.

Recently, Yang and Gunasekaran[5] made a comparison between the predictions of Lambert's law—Eq. 13 with no matching procedure and constant dielectric properties—and Maxwell's law for the temperature distribution in a cylindrical sample (assumed radially irradiated). The power adsorption pattern between the two laws is very different for the cases under consideration, and the temperature predictions using Maxwell's law are clearly better than those using Lambert's law.

Nonuniform dielectric properties

Let us next examine what happens in the case of temperature-dependent properties. The dielectric properties of water at $f = 2750$ MHz are considered again. Their temperature dependency in the range 20–80°C is derived from the figures given by Ryyananen et al.[14] The temperature profile is assumed to be linear in r with a minimum temperature $T_{\min} = 20$°C and a maximum temperature $T_{\max} = T_{\min} + DT$. The minimum temperature can be located at the circumference (case 1) or at the axis (case 2) of the cylinder. The normalized exact heat source can be found by substituting the solution of the boundary-value problem (BVP, Eqs. 1–5) in Eqs. 9 and 18. The above linear temperature profile seems rather unreasonable, although one should keep in mind that the scope here is not to simulate the heating process but to establish criteria for the use of simplified expressions for the heat source. Taking into account that the number of parameters must be kept at a minimum, the linear temperature profile comes naturally as the best choice. With respect to objections about the unrealistic finite slope of the linear profile at $r = 0$ one is reminded that the approximate expressions under consideration also predicts a finite slope. In any case, a small variation of the linear profile to accommodate the zero slope at $r = 0$ would have absolutely no influence on the results and conclusions of the present work.

In Figures 2a and 2b the normalized heat generation distribution is shown for case 1 with $\beta_{r=R}R = 3$ and $DT = 10$ and 30°C, respectively. The notation $\beta_{r=R}$ denotes the value of β computed at the temperature of the point $r = R$. It is shown that as DT increases the temperature rise in the cylinder leads to lower values of β and a higher degree of oscillation close to the cylinder axis. The approximation Q_4 is obviously better than Q_2. To assess the approximation with respect to the temperature variation, the normalized errors N_2 and N_4 are presented in Figure 3 with respect to the temperature difference DT for the case 1 and for $\beta_{r=R}R = 3$, 4, and 5. For both approximations the error increases as $\beta_{r=R}R$ decreases and DT increases, as

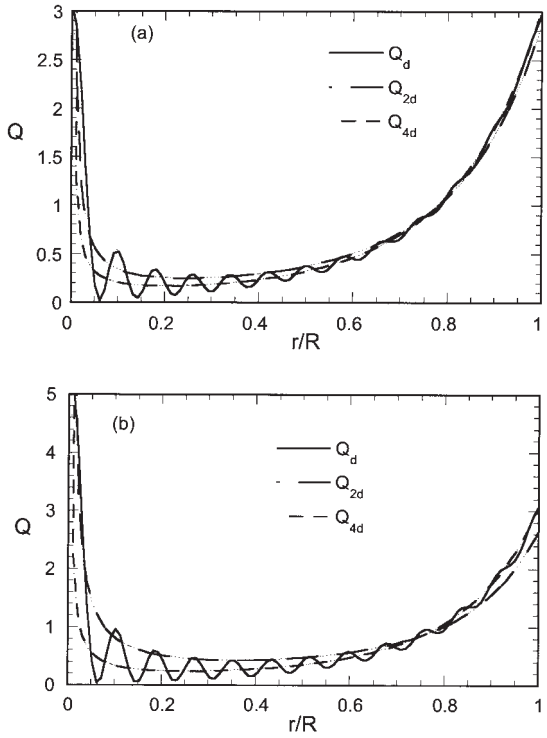

Figure 2. Exact and approximate normalized distribution of the heat source for $\beta_{r=R}R = 3$.

Water at $f = 2750$ MHz, case 1 temperature profile: (a) $DT = 10$°C; (b) $DT = 30$°C.

expected. This error arises from the oscillating nature of the exact solution, which cannot be followed by the approximate one. The error is larger for the Q_2 approximation and it is almost independent from the value $\beta_{r=R}R$ for large DT. In this case, the source of error is not only the oscillations of the exact solution but also the inability of the approximation to reproduce solutions (even nonoscillating) with varying dielectric properties. This argument is further confirmed by Figure 4 (case 2, $DT = 30$°C, $\beta_{r=R}R = 2.5$), where it is clear that even a smooth exact solution (which can be approximated with very high accuracy by Q_4) cannot be reproduced by Q_2.

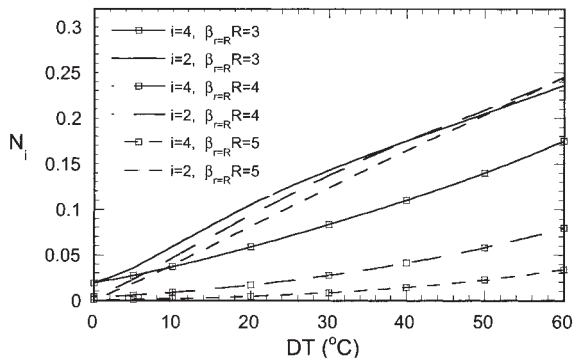

Figure 3. Normalized errors of the approximate expressions for the heat source distribution vs. DT for several values of $\beta_{r=R}R$.

Water at $f = 2750$ MHz, case 1 temperature profile.

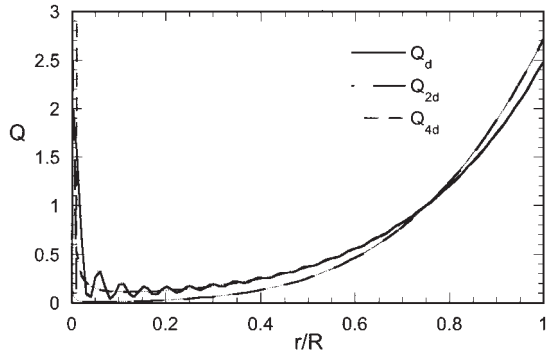

Figure 4. Exact and approximate normalized distribution of the heat source for $\beta_{r=R}R = 2.5$ and $DT = 30$°C.

Water at $f = 2750$ MHz, case 2 temperature profile.

For the case 2 temperature profile, as DT increases βR inside the cylinder decreases, leading to suppression of the oscillations of the heat generation distribution. This means better performance of the approximation Q_4 as DT increases, keeping the quantity $\beta_{r=R}R$ constant. Actually, the error of the approximation is determined by the value βR at the region that is more susceptible to oscillations (axis of the cylinder). For Figure 4, this value is $\beta_{r=0}R = 5$ and that is why Q_4 performs well. The immediate conclusion emerging from the above analysis is that the approximate expression Q_4 can be safely used for a heat generation profile during the radial irradiation of a cylindrical sample, with an error estimated by Eq. 25 using $\beta_{r=0}R$.

To this end, there are actually two methods for the computation of the heat source term for the radial irradiation of a cylindrical sample: the approximation Q_4 or the solution of Eqs. 1–5 and 9. The above equations must be solved numerically at each time step of the heating process so the use of Q_4 is more desirable. To decide whether Q_4 is appropriate, the constant β that corresponds to the maximum estimated temperature at the axis of the sample must be computed; this value of β can then be used for an estimation of the error in Q_4, from Eq. 25. Depending on this error, the approximation Q_4 can or cannot replace the complete equations for the electric field. A criterion proposed here is $\beta_{r=0}R \geq 3$. This criterion can be generalized for β's spatial dependency attributed not only to temperature but also to composition[15] or structure.[16] In any case, the above criterion must be fulfilled with the β value computed at $r = 0$.

It is worth noting that, to obtain the heat source distribution shown in Figure 2b, the algorithm returns 116 discretization points for a relative error of 10^{-4} and 42 points for a relative error of 10^{-2}. Considering the high order of the numerical method of integration and the unequal (optimum) spacing, a much larger number of discretization points is needed for a comparable accuracy with the second-order finite-element method with equal spacing (usually used in the literature for the particular problem[16]). Decoupling the heat-transfer equation from the microwave radiation equations and solving a BVP for the latter at each time step of the former (equivalent to a moving grid approach) seems to be a tempting alternative to the combined solution using a finite-element discretization.

Conclusions

In modeling the microwave heating of a radially irradiated cylindrical sample (for constant dielectric properties) the simplified relation expressed in Eq. 13 for the heat source can be used instead of the exact analytical solution of Maxwell's equation[7] if $\beta R \geq 3$. The main advantage of using Eq. 13 is that it permits easier analytical manipulation in case of solving the heat-transfer equation using analytical and asymptotic techniques. For temperature-dependent dielectric properties, the criterion for using relation 15 instead of numerically solving the Maxwell equations is $\beta_{r=0} R > 3$. The parameter β must be computed at the center of the cylinder. In this case, the advantage of using Eq. 15 is that the solution of the Maxwell equations coupled with the heat-transfer equation—increasing the computational effort many times!—is avoided.

Literature Cited

1. Ayappa KG, Davis HT, Davis EA, Gordon J. Two dimensional finite element analysis of microwave heating. *AIChE J.* 1992;38:1577-1592.
2. Fleischman GJ. Predicting temperature range in food slabs undergoing long term/low power microwave heating. *J Food Eng.* 1996;27:337-351.
3. Fleischman GJ. Predicting temperature range in food slabs undergoing short term/high power microwave heating. *J Food Eng.* 1999;40:81-88.
4. Vilayannur RS, Puri VM, Anantheswaran RC. Size and shape effect on nonuniformity of temperature and moisture distributions in microwave heated food materials: Part I. Simulation. *J Food Proc Eng.* 1998;21:209-233.
5. Yang HW, Gunasekaran S. Comparison of temperature distribution in model food cylinders based on Maxwell's equations and Lambert's law during pulsed microwave heating. *J Food Eng.* 2004;64:445-453.
6. Ayappa KG, Davis HT, Crapiste G, Davis EA, Gordon J. Microwave heating: An evaluation of power formulations. *Chem Eng Sci.* 1991;46:1005-1016.
7. Oliveira MEC, Franca AS, Microwave heating of foodstuffs. *J Food Eng.* 2003;53:347-359.
8. Press WH, Teukolsky SA, Vetterling WT, Flannery BP. *Numerical Recipes: The Art of Scientific Computing*. New York, NY: Cambridge Univ. Press; 1992.
9. Chen DSD, Singh RK, Haghighi K, Nelson PE. Finite element analysis of temperature distribution in microwaved cylindrical potato tissue. *J Food Eng.* 1993;18:351-368.
10. Lin YE, Anantheswaran RC, Puri VM. Finite element analysis of microwave heating of solid foods. *J Food Eng.* 1994;25:85-112.
11. Rattanadecho P. Theoretical and experimental investigation of microwave thawing of frozen layer using a microwave oven (effect of layered configuration and layer thickness). *Int J Heat Mass Transfer.* 2004;7:937-945.
12. Barringer SA, Davis EA, Gordon J, Ayappa KG, Davis HT. Microwave-heating temperature profiles for thin slabs compared to Maxwell and Lambert law predictions. *J Food Sci.* 1995;60:1137-1142.
13. Sakonidou EP, Karapantsios TD, Raphaelides SN. Mass transport limitations during starch gelatinization. *Carbohydr Polym.* 2003;53:53-61.
14. Ryyananen S, Risman PO, Ohlsson T. The dielectric properties of native starch solutions—A research note. *J Microwave Power Electromagn Energy* 1996;31:50-53.
15. Basak T. Role of resonances on microwave heating of oil–water emulsions. *AIChE J.* 2004;50:2569-2675.
16. Chatterjee A, Basak T, Ayappa KG. Analysis of microwave sintering of ceramics. *AIChE J.* 1998;44:2302-2311.

Manuscript received Jan. 21, 2005, and revision received May 16, 2005.